JOURNAL OF SOLID STATE CHEMISTRY **135,** 159–168 (1998)
ARTICLE NO. SC977618

Orthorhombic WO_3 Formed via a Ti-Stabilized $WO_3 \cdot \frac{1}{3}H_2O$ Phase

B. Pecquenard,* H. Lecacheux,* J. Livage,*,[1] and C. Julien†

*Laboratoire de Chimie de la Matière Condensée and †Laboratoire des Milieux Désordonnés et Hétérogènes, Université Pierre et Marie Curie, 4 place Jussieu, 75252 Paris, France

Received May 7, 1997; in revised form September 3, 1997; accepted September 9, 1997

Stable solutions of WO_3 precursors have been prepared via the dissolution of tungstic acid, H_2WO_4, in hydrogen peroxide. A crystalline peroxopolytungstic acid $WO_3 \cdot H_2O_2 \cdot nH_2O$ ($n \approx 0.1$) is obtained upon drying. Peroxo groups decompose at 200°C, giving an amorphous tungsten oxide that crystallizes into the stable monoclinic WO_3 around 400°C. Completely different results are obtained when $Ti(OPr^i)_4$ is added to the precursor solution. The orthorhombic phase $WO_3 \cdot \frac{1}{3}H_2O$ is first obtained. As is well known, this hydrated oxide leads to h-WO_3 and m-WO_3 upon heating. However, in the presence of Ti^{IV}, a new metastable orthorhombic tungsten oxide is formed around 400°C. It then transforms irreversibly upon further heating into the stable monoclinic WO_3. The presence of Ti^{IV} seems to stabilize this new orthorhombic phase. © 1998 Academic Press

INTRODUCTION

A large number of tungsten oxides have been described in the literature (1). Crystalline tungsten oxides exhibit ReO_3-type structures based on corner-sharing [WO_6] octahedra (2). Due to the displacement of W^{6+} ions, these octahedra are more or less distorted. The type and magnitude of these distortions depend on temperature, giving rise to several polymorphic forms (tetragonal, orthorhombic, monoclinic, and triclinic) which transform reversibly into each other as a function of temperature. Not less than eight phase transformations have been reported up to 1000°C for stoichiometric tungsten trioxide (3).

Several hydrated tungsten oxides $WO_3 \cdot nH_2O$ have also been described. They are built from corner-sharing [WO_6] or [$WO_5(OH_2)$] octahedra. Following the pioneering work of Figlarz *et al.* (4), metastable tungsten oxides have been obtained from these hydrated phases via "chimie douce." The orthorhombic oxide $WO_3 \cdot \frac{1}{3}H_2O$ is obtained via the hydrothermal treatment of tungstic acid $H_2WO_4 \cdot H_2O$. Upon thermal dehydration around 300°C it leads to the hexagonal oxide h-WO_3. A supermetastable orthorhombic WO_3 phase, with the same structure as the hydrate, has even been reported (5). The dehydration of $WO_3 \cdot 2H_2O$ leads to $WO_3 \cdot H_2O$ and then to a cubic WO_3 with a perfect ReO_3 structure (6). Tungsten oxides with a pyrochlore-type structure have also been obtained via the thermal decomposition of ammonium tungstate (7, 8). Upon further heating around 400°C, all these metastable oxides lead to the stable monoclinic WO_3 phase.

Tungsten oxide is a well-known electrochromic material. Its coloration switches reversibly from white to blue upon the electrochemical insertion of monovalent cations such as Li^+ or H^+ (9). Several authors have shown that reversibility can be improved by adding TiO_2 to the tungsten oxide. The lifetime of WO_3–TiO_2 thin films can be five times longer than that of pure WO_3 (10, 11). Therefore several studies have been undertaken to obtain more information on the structure and electrochemical properties of WO_3–TiO_2 thin films (12).

This paper reports on the synthesis of WO_3–TiO_2 oxide phases from aqueous solutions in the presence of hydrogen peroxide. It shows that adding small amounts of Ti^{IV} to the precursor solution strongly changes the nature of the crystalline tungsten oxide phases. A new metastable orthorhombic phase has even been observed during the thermal treatment of hydrated WO_3–TiO_2 oxides.

EXPERIMENTAL TECHNIQUES

Precursor solutions and oxide powders were characterized using the following experimental techniques.

^{183}W NMR experiments were performed on aqueous solutions with a Bruker MSL 400 spectrometer. Chemical shifts were measured using Na_2WO_4 (2 M) or [$H_4SiW_{12}O_{40}$] solutions in D_2O as a reference. As the sensitivity of the ^{183}W nucleus is very weak (natural abundance 14.4%, $\gamma = 1.12 \times 10^7$ rad $\cdot T^{-1} \cdot s^{-1}$), NMR spectra had to be accumulated for more than 24 h (> 5000 scans).

Phase identification of powders was carried out by X-ray diffraction with a Philips diffractometer equipped ($CuK\alpha_1$, $\lambda = 1.540598$ Å) in reflection geometry.

Infrared absorption spectra were recorded on powders dispersed in KBr pellets using a Fourier transform Nicolet

[1] To whom correspondence should be addressed.

0022-4596/98 $25.00
Copyright © 1998 by Academic Press
All rights of reproduction in any form reserved.

spectrometer working between 500 and 4000 cm^{-1}. Raman scattering was measured in the frequency range 10–1200 cm^{-1} with a Jobin-Yvon U-1000 double monochromator using the 514.5-nm line of a Spectra Physics argon ion laser for excitation. A low laser power of 50 W/cm^2 was used to avoid any thermally induced transformation or decomposition of hydrated compounds.

Thermal analyses of the powders were performed with a Netzsch STA 409 thermal analyzer under an oxygen atmosphere and at a heating rate of 5°C/min.

RESULTS AND DISCUSSION

Solutions of Molecular Precursors

Synthesis of stable solutions. Thin films of amorphous WO_3 can be deposited from aqueous solutions of tungstic acid (13). These solutions are prepared via the acidification of aqueous solutions of sodium tungstate, Na_2WO_4, through a proton exchange resin (13). A clear solution of tungstic acid is first obtained, but these solutions are not stable; condensation reactions occur spontaneously, leading to the precipitation of hydrated tungsten oxides $WO_3 \cdot nH_2O$ ($n = 1$ or 2). Such solutions are therefore not convenient for the deposition of optically transparent thin films and the realization of electrochromic devices. Therefore another route was chosen. As shown by Kudo *et al.* (14, 15), stable solutions of peroxotungstic acid can be obtained via the dissolution of W or WC in aqueous solutions of hydrogen peroxide. The following procedure was therefore used:

Pure "WO_3" samples were obtained via the dissolution of commercial tungstic acid, $WO_3 \cdot H_2O$, in aqueous solutions of H_2O_2 (30%). A clear solution of peroxotungstic acid is obtained (tungsten concentration $\approx 0.6\ mol \cdot L^{-1}$). This solution is strongly acid (pH 1.7) and remains stable for months, as long as H_2O_2 in excess is not removed (16).

Mixed "WO_3–TiO_2" samples were formed by slowly adding titanium isopropoxide, $Ti(OPr^i)_4$, to the previous solution in an iced-cooled-beaker. The solution immediately turns yellow, orange, and red. Such colors are typical of the formation of peroxotitanate species $[Ti(O_2)(OH)_{n-2}]^{(4-n)+}$ in which Ti^{4+} ions are complexed by bidentate $[O_2]^{2-}$ ligands (17). Condensation reactions are prevented by the protonation (pH < 2) and complexation of titanium molecular precursors, avoiding the precipitation of TiO_2, and the solution remains clear. Different solutions have been prepared containing up to 5 mol% of titanium. The stability of these peroxo solutions decreases when the amount of Ti increases, but solutions containing 5% of Ti can be kept for 2 months before precipitation occurs.

^{183}W NMR of the precursor solutions. The ^{183}W NMR spectrum of a pure peroxotungstic solution ([W] = 0.6 M) exhibits only two peaks, at -696.5 and -631.2 ppm (Fig. 1a), that can be assigned to molecular peroxotungstic species such as $[W_2O_3(O_2)_4(H_2O)_2]^{2-}$ (18). This ^{183}W NMR spectrum does not change significantly when the solution is aged under ambient conditions, both peaks are still visible after several weeks.

The ^{183}W NMR spectra of the solution changes as soon as $Ti(OPr^i)_4$ is added. The two peaks corresponding to peroxotungstic species progressively disappear when the solution is aged for several days while new peaks are observed at less negative chemical shift values (Fig. 1b). The peak at -179 ppm can be assigned to oxotungstate species that do not contain any peroxo ligand, whereas the two peaks at -525 and -481 ppm should correspond to intermediate oxo–peroxo species (19).

Hydrated Oxide Powders

The peroxo solutions are very stable and precipitation is not observed even after 2 or 3 months. Powders were therefore obtained via the slow evaporation of the solution around 60°C in a humid atmosphere. A white powder precipitates from pure peroxotungstic acid solutions, whereas powders obtained from mixed W–Ti solutions still exhibit an orange coloration. All these powders are then filtered from the solution and dried at room temperature.

X-ray diffraction. The white powders obtained from pure peroxopolytungstic acid solutions are well crystallized (Fig. 2a). Their X-ray diffraction pattern corresponds to the $WO_3 \cdot H_2O_2 \cdot nH_2O$ ($n \approx 0.14$) phase described by Kudo *et al.* (20).

Crystalline powders are still obtained from mixed "W–Ti" solution. However, their X-ray diffraction pattern is completely different and these phases appear to be isotypes of the well known orthorhombic hydrated oxide $WO_3 \cdot \frac{1}{3}H_2O$ (Fig. 2b).

Infrared and Raman spectroscopies. The infrared spectrum of "WO_3" powders exhibits the low-frequency absorption bands typical of W=O (968 cm^{-1}) and W–O–W (650 cm^{-1}) together with those corresponding to peroxo groups O–O bonded to tungsten at 903 cm^{-1} and the tungsten–peroxo bonds at 540 cm^{-1}. Absorption bands due to water molecules can also be seen at higher frequencies, around 3400 and 1600 cm^{-1} (Fig. 3a).

The infrared spectrum of "WO_3–TiO_2" mixed powders still exhibits the absorption bands of water molecules, but the low-frequency part corresponding to metal–oxygen vibrations is significantly different (Fig. 3b). The vibration bands typical of peroxotungstic groups are no longer visible and only a broad and poorly resolved band corresponding to the $WO_3 \cdot \frac{1}{3}H_2O$ phase can be seen between 500 and 1000 cm^{-1} (21).

The Raman spectrum of the orthorhombic $WO_3 \cdot \frac{1}{3}H_2O$ compound obtained in the presence of Ti^{IV} is much better resolved (Fig. 6). It exhibits a strong peak located at

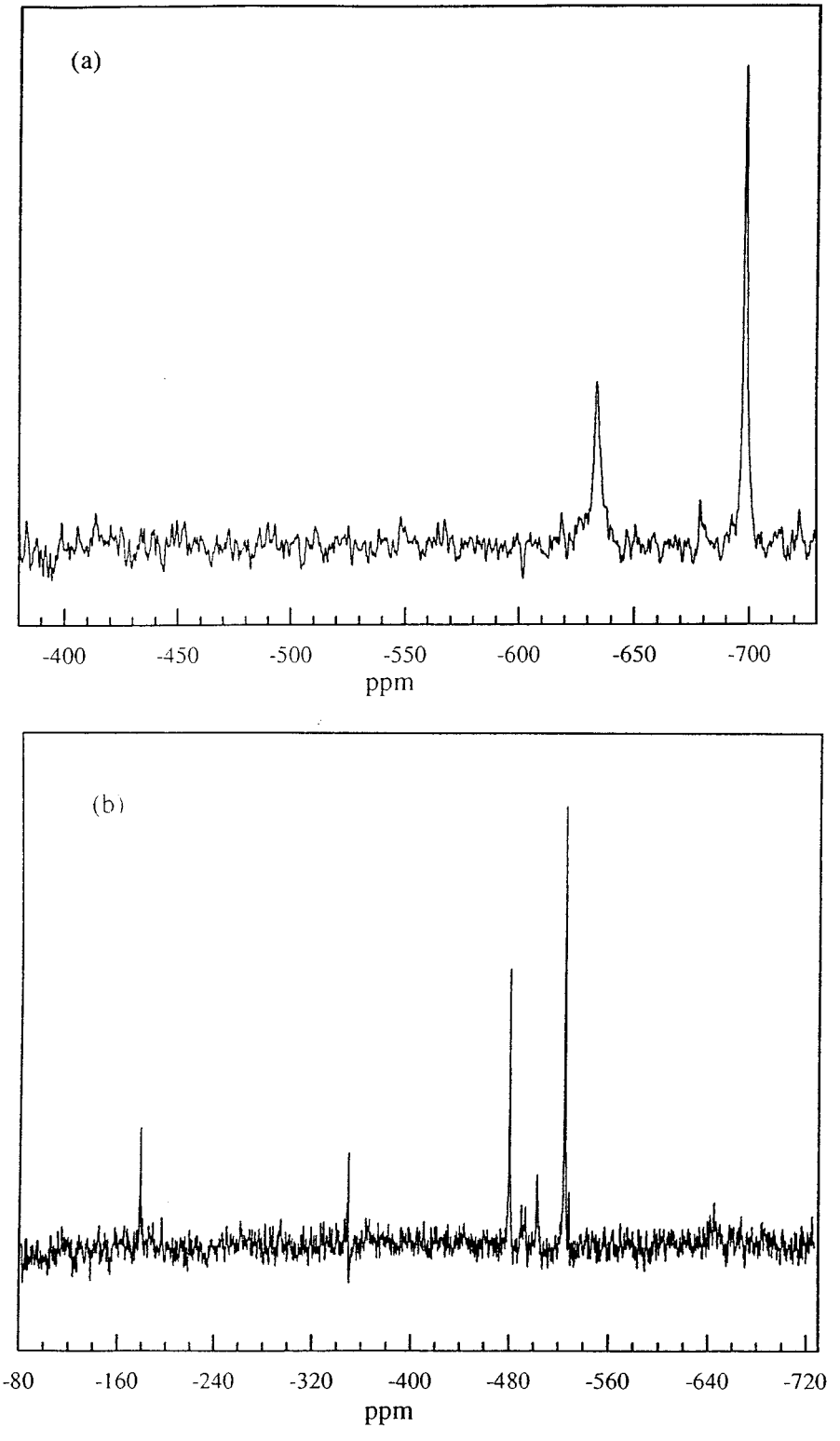

FIG. 1. ^{183}W NMR spectra of precursor solutions in H_2O_2: (a) peroxopolytungstic acid; (b) solution containing W and Ti (2 mol%).

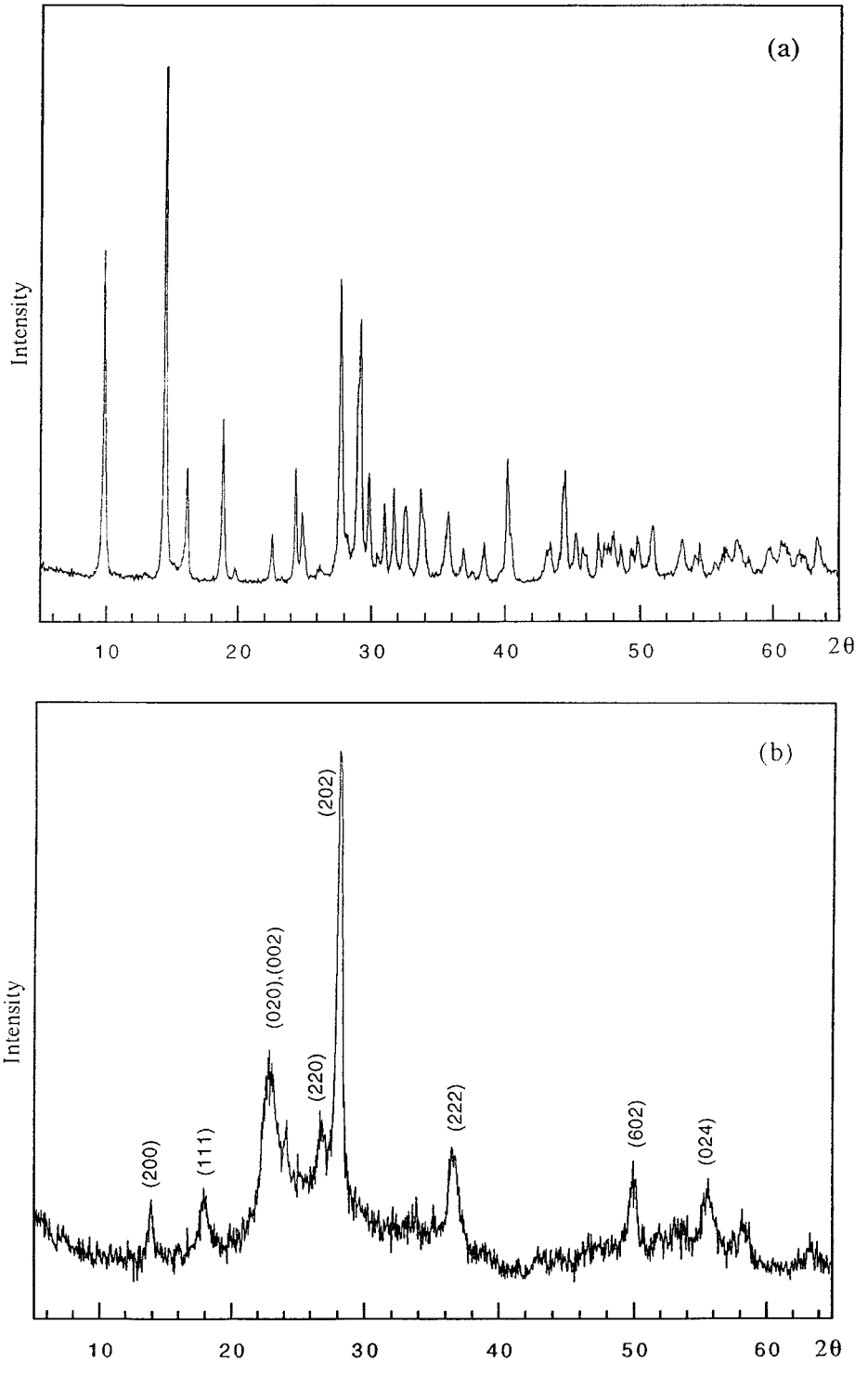

FIG. 2. X-ray diffraction spectra of hydrated oxides: (a) $WO_3 \cdot H_2O_2 \cdot 0.14H_2O$ from pure W solutions; (b) $WO_3 \cdot \frac{1}{3}H_2O$ from mixed W–Ti solutions.

69 cm^{-1}, a broad band centered at 237 cm^{-1}, and three well-resolved bands at 679, 805, and 951 cm^{-1}. The two-dimensional character of $WO_3 \cdot \frac{1}{3}H_2O$ can be pointed out from the width of the bands situated at 679 and 805 cm^{-1}, which are assigned to stretching vibrations ν(W–O–W) of the bridging oxygen atoms. The band located at 951 cm^{-1} is attributed to the stretching mode of the terminal W=O double bond (Table 1).

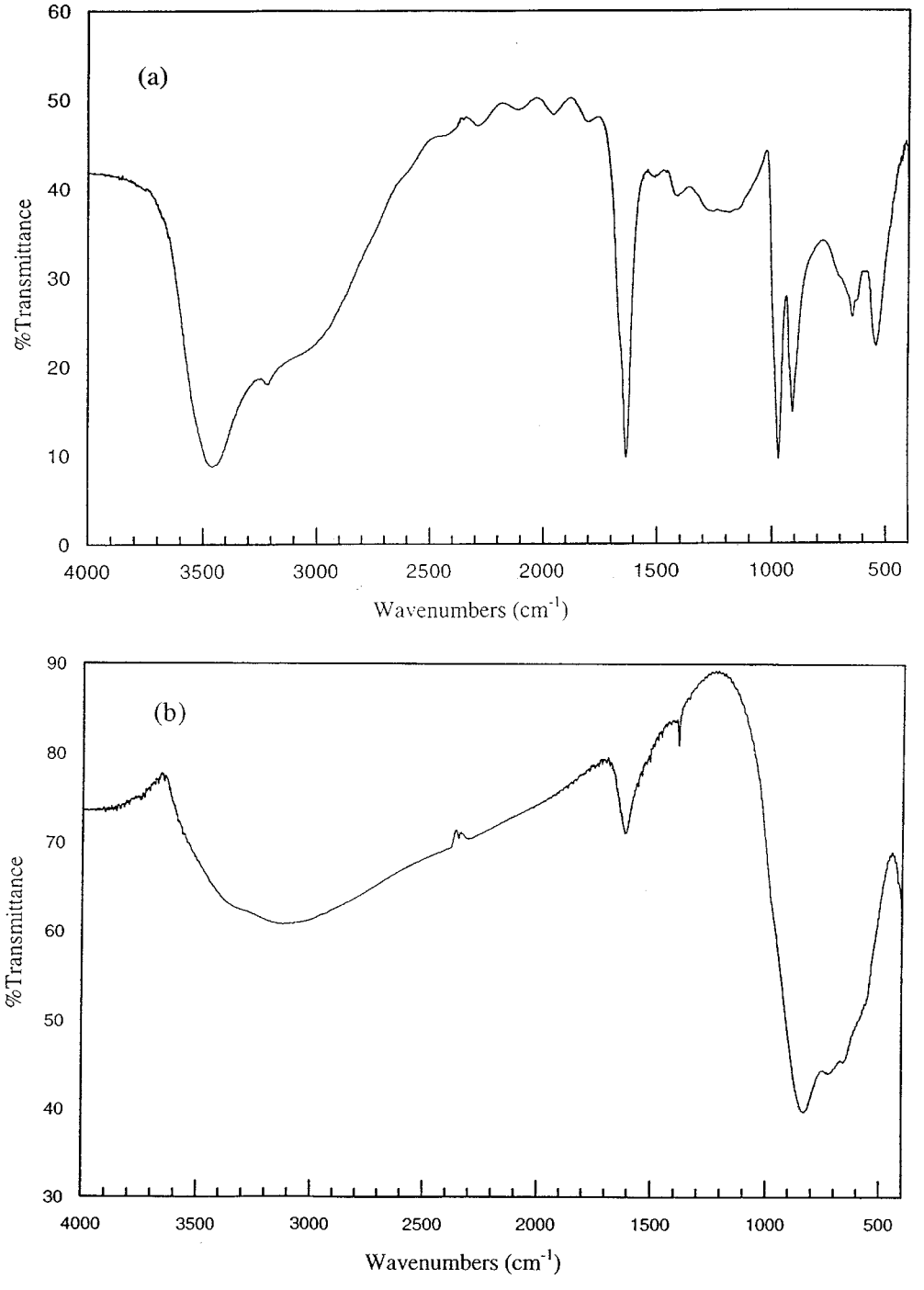

FIG. 3. Infrared absorption spectra of hydrated oxide powders. (a) $WO_3 \cdot H_2O_2 \cdot 0.14H_2O$ from pure W solutions; (b) $WO_3 \cdot \frac{1}{3}H_2O$ from mixed W–Ti solutions.

Thermal Treatment of Hydrated Oxides

As-prepared samples correspond to crystalline hydrated oxides. Dehydration therefore occurs upon heating, leading to oxide phases.

The thermal analysis curve of the peroxo phase $WO_3 \cdot H_2O_2 \cdot nH_2O$ obtained from pure "WO_3" solutions exhibits a very small endothermic weight loss corresponding to the departure of about $0.1H_2O$ per WO_3 below 170°C followed by the decomposition of peroxo groups ($[O_2]/[W] \approx 1$) at

TABLE 1
Characteristic Raman Frequencies (in cm^{-1}) of the Four WO_3 phases

$WO_3 \cdot \frac{1}{3}H_2O$	h-WO_3	o-WO_3	m-WO_3	Assignment
			33	
		45	44	
53	57	61	60	
69	64		71	
		77	83	$\nu(W_2O_2)_n$
		91	94	
113	116			
	138	143	143	
		179	182	
		203		
237			242	
		253		
278	274	271	273	δ(O–W–O)
		303		
335			326	
		374		
	654	636	638	
679	691	713	716	ν(O–W–O)
805	805	807	806	
951	950			ν(W=O)

200°C (Fig. 4a). An amorphous oxide is then obtained and the exothermic crystallization occurs at 390°C, leading to the stable monoclinic tungsten oxide.

The thermal behavior of mixed "WO_3–TiO_2" hydrated phases is completely different. Two weight losses are observed corresponding to the departure of adsorbed water up to 200°C ($H_2O/WO_3 \approx 1$) and bound water ($H_2O/WO_3 = 0.33$) between 200 and 400°C (Fig. 4b).

X-ray diffraction experiments performed on samples heated for 1 h at different temperatures show that several crystalline phases are successively formed (Fig. 5). No amorphous phase is observed during the thermal treatment after dehydration. $WO_3 \cdot \frac{1}{3}H_2O$ directly gives the well-known metastable hexagonal WO_3. This phase usually transforms into the stable monoclinic oxide above 400°C. This is not the case here, the monoclinic phase is actually observed at higher temperature (≈ 1000°C). X-ray diffraction shows the formation of a new metastable WO_3 phase above 500°C. This phase is orthorhombic and the lattice parameters calculated from the powder X-ray diffraction diagram lead to $a = 7.39$ Å, $b = 7.51$ Å, and $c = 3.83$ Å. Upon further thermal treatment at higher temperature, some phase segregation occurs, leading to the formation of TiO_2 and monoclinic WO_3.

Raman scattering confirms the formation of this new orthorhombic phase. Figure 6 gives the Raman spectra corresponding to the different crystalline phases obtained after thermal treatment, i.e., hydrated tungsten oxide ($WO_3 \cdot \frac{1}{3}H_2O$) and the hexagonal (h-$WO_3$), orthorhombic (o-$WO_3$), and monoclinic (m-$WO_3$) tungsten trioxides. Several observations can be pushed forward:

(i) These spectra exhibit marked differences. This reflects the crystal structures which lead to some frequency shift and an increasing number of peaks when the symmetry decreases.

(ii) Three-dimensional structures such as o-WO_3 give narrower lines and the W=O vibration around 950 cm^{-1} disappears.

(iii) All these spectra exhibit some similar features. The high-frequency band (806 cm^{-1}) for instance, due to the O–W–O stretching mode (tungsten oxide network), can be seen in all samples.

(iv) The different bands can be classified in three groups according to the frequency range. The external motions of one [WO_6] unit, considered as an isolated pseudomolecule, are expected to occur in the low-wavenumber region. The internal modes, described in terms of W–O bending and stretching vibrations, are related to the medium- and the high-frequency bands, respectively. These vibrational modes, estimated for the monoclinic symmetry, are closely related with those of the orthorhombic and hexagonal phases. They can be compared with Raman data of the various powder samples of WO_3 in their hydrated and anhydrous forms reported by Daniel *et al.* (21).

CONCLUSION

As reported earlier, peroxopolytungstic acids are formed when a tungsten compound is dissolved in an aqueous solution of hydrogen peroxide. The slow evaporation of these solutions gives a crystalline powder corresponding to $WO_3 \cdot H_2O_2 \cdot 0.14H_2O$ in which peroxo groups remain bonded to W^{VI}. The structure of this phase has not yet been determined. Upon thermal decomposition it leads to an amorphous oxide and then to the usual monoclinic WO_3 (m-WO_3).

Adding small amounts of titanium ($< 5\%$) to the solution of peroxopolytungstic acid dramatically changes its behavior. Ti^{IV} reacts readily with peroxo ligands, giving strongly colored complexes. The well-known hydrated oxide $WO_3 \cdot \frac{1}{3}H_2O$ is then obtained even without any hydrothermal treatment. Similar results have been reported recently in the V–W–O system. Adding V_2O_5 to the H_2O_2 solution also leads to the formation of $WO_3 \cdot \frac{1}{3}H_2O$ (22, 23). The orange coloration of the crystalline powder suggests that peroxotitanate groups are still adsorbed at the surface of, or trapped within, the hydrated tungsten oxide powder. However, the amount of Ti is too small to lead to measurable variations of the cell parameters.

Dehydration occurs upon heating, giving the usual hexagonal and monoclinic WO_3 oxides. However, a new metastable orthorhombic phase is formed between 500 and

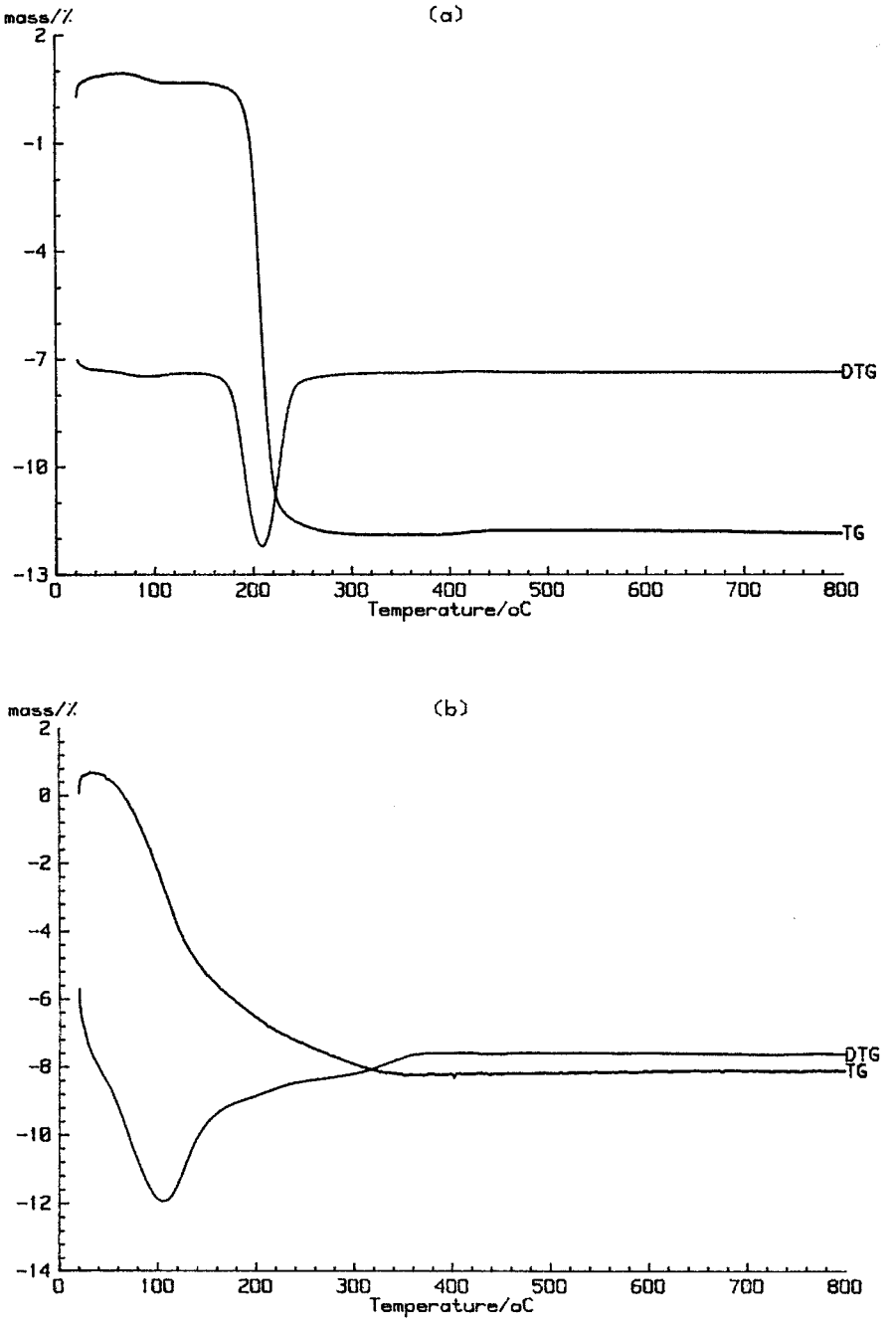

FIG. 4. Thermal analyses of hydrated powders (TG = thermogravimetry, DTG = differential thermogravimetry): (a) $WO_3 \cdot H_2O_2 \cdot 0.14H_2O$ from pure W solutions; (b) $WO_3 \cdot \frac{1}{3}H_2O$ from mixed W–Ti solutions.

900°C. This phase cannot be obtained in the absence of titanium, but even small amounts of Ti^{IV} ($\approx 2\%$) lead to o-WO_3. It is very difficult to obtain a pure metastable o-WO_3 phase. It is always mixed with some m-WO_3. Moreover, X-ray diffraction patterns are not sharp enough to allow the structural determination of this orthorhombic phase that seems to be isostructural with the high-temperature orthorhombic phase already observed by Roth *et al.* in WO_3–Nb_2O_5 (98%–2%) solid solutions (24).

Raman scattering experiments confirm the formation of this new phase and provide some structural information. The Raman spectra of tungsten oxides have already been analyzed in the literature. The lattice dynamics of tetragonal WO_3 was investigated by Salje (25) whereas the concept of

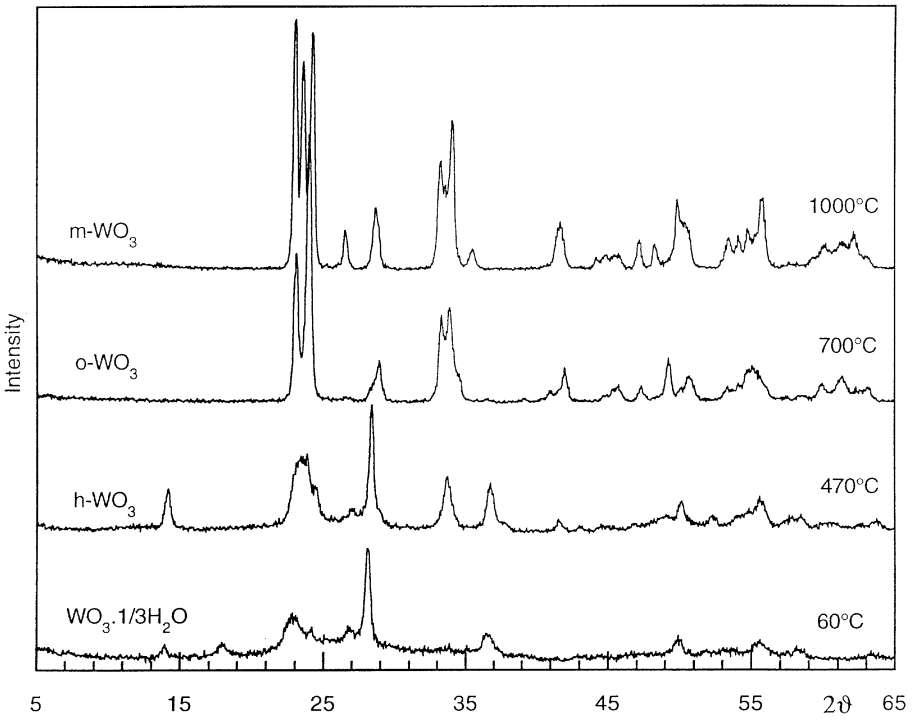

FIG. 5. X-ray diffraction pattern of mixed "WO_3 (95%)–TiO_2 (5%)" powders heated at different temperatures.

group frequency was applied to the vibrational spectra of oxides (26). Tungsten trioxide exhibits several phases that can be all considered as distorted forms of the ideal ReO_3-type structure. The structural relationships between $WO_3 \cdot \frac{1}{3}H_2O$, h-$WO_3$, o-$WO_3$, and m-$WO_3$ can be deduced from Raman scattering measurements. The analysis is based on the well-known fact that tungsten trioxides are built from $[WO_6]$ octahedra in which the W–O stretching and bending vibrations always occur in the 950–600- and 400–200-cm^{-1} regions, respectively (21). As already established (4, 25, 26), the distortion of the octahedra and the considerable lowering of the symmetry in the monoclinic form, m-WO_3, lead to a greater number of active modes compared with the hexagonal and orthorhombic forms. Thus the Raman scattering spectrum of m-WO_3 develops well-resolved low-wavenumber peaks at 33, 44, 60, 71, 83, and 94 cm^{-1}, which are attributed to the vibrational modes due to $(W_2O_2)_n$ chains.

Important modifications can be observed between the different crystalline WO_3 phases in the low-wavenumber region, showing the importance of bond lengths and angles in these crystals. A comparison of the Raman spectra of the four WO_3 phases (Fig. 6) suggests that the structural transformations from hexagonal to monoclinic WO_3 via the new orthorhombic WO_3 phase involve modifications in W–O arrangements. The low-frequency part of the Raman scattering spectrum of m-WO_3 shows that corner-sharing octahedra are connected in such a way that isolated pseudo-molecules are vibrating in-phase, giving rise to narrow bands. These specific connections disappear in orthorhombic WO_3 because of some change in the distribution of bond angles between $[WO_6]$ octahedra. This could be due to the formation of some edge-sharing octahedra, in addition to the usual corner-sharing octahedra. Such an assumption is in agreement with the structural model proposed by Harb *et al.* (27).

Tungsten oxides WO_3 and hydrates $WO_3 \cdot nH_2O$ are built up of corner-sharing $[WO_6]$ or $[WO_5(OH_2)]$ octahedra (1). Edge-sharing octahedra are only seen in tungstate compounds. The metastable orthorhombic phase, more symmetric than the monoclinic one, has never been observed in pure WO_3. It appears that some Nb^{5+} or Ti^{4+} ions, less polarizing than W^{6+}, are required to stabilize the o-WO_3 phase at room temperature. According to a recent work published by Depero *et al.* (12), symmetries higher than monoclinic m-WO_3 may result from the introduction of some static disorder which can be ascribed to the presence of randomly distributed clusters of edge-sharing $[WO_6]$ octahedra. Actually, the presence of such edge-sharing octahedra is suggested by our analysis of the Raman spectrum of o-WO_3. Edge-sharing could be favored by the substitution of W^{6+} by Ti^{4+} ions, which have a lower oxidation state, decreasing electrostatic repulsion between adjacent cations.

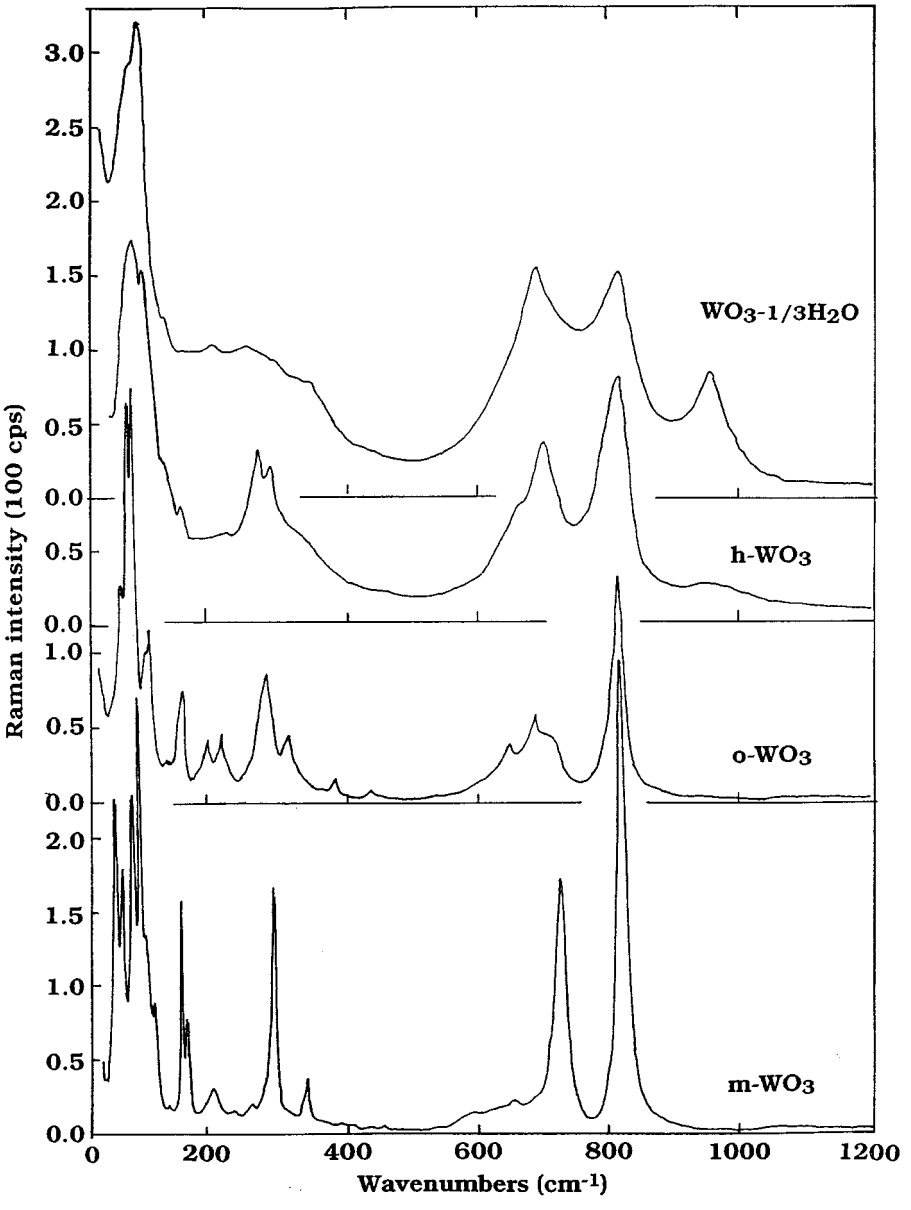

FIG. 6. Raman scattering spectra of mixed "WO_3 (95%)–TiO_2 (5%)" crystalline powders heated at different temperatures: 60°C ($WO_3 \cdot \frac{1}{3}H_2O$), 470°C (h-$WO_3$), 700°C (o-$WO_3$), and 1000°C (m-$WO_3$).

ACKNOWLEDGMENTS

The authors thank G. Guzman for helpful discussions and R. Thouvenot for the ^{183}W NMR spectra.

REFERENCES

1. B. Gérand and L. Seguin, *Solid State Ionics* **84,** 199 (1996).
2. A. F. Wells, "Structural Inorganic Chemistry." Oxford University Press, Oxford, 1984.
3. I. Levkowitz, M. B. Dowell, and M. A. Shield, *J. Solid State Chem.* **15,** 24 (1975).
4. B. Gérand, G. Nowogrocki, and M. Figlarz, *J. Solid State Chem.* **38,** 312 (1981).
5. L. Seguin, M. Figlarz, and J. Pannetier, *Solid State Ionics* **63–65,** 437 (1993).
6. O. Yamaguchi, D. Tomihisa, H. Kawabata, and K. Shimizu, *J. Am. Ceram. Soc.* **70,** C94 (1987).
7. A. Coucou and M. Figlarz, *Solid State Ionics* **28–30,** 1762 (1988).
8. R. Nedjar, M. Borel, M. Hervieu, and B. Raveau, *Mater. Res. Bull.* **23,** 91 (1988).
9. C. G. Granqvist, "Handbook of Inorganic Electrochromic Materials." Elsevier, Amsterdam, 1995.
10. S. Hashimoto and H. Matsuoka, *J. Electrochem. Soc.* **138,** 2403 (1991).
11. S. Hashimoto and H. Matsuoka, *Surface Interface Anal.* **19,** 464 (1992).

12. L. E. Depero, S. Groppelli, I. Natali-Sora, L. Sanfgaletti, G. Sberveglieri, and E. Tondello, *J. Solid State Chem.* **121,** 379 (1996).
13. A. Chemseddine, R. Morineau, and J. Livage, *Solid State Ionics* **9–10,** 357 (1983).
14. T. Kudo, *Nature* **312,** 537 (1984).
15. T. Kudo, H. Okamoto, K. Matsumoto, and Y. Sasaki, *Inorg. Chim. Acta* **111**, L27 (1985).
16. J. Livage and G. Guzman, *Solid State Ionics* **84,** 205 (1996).
17. J. Mühlebach, K. Müller, and G. Schwarzenbach, *Inorg. Chem.* **9,** 2381 (1970).
18. M. H. Dickman and M. T. Pope, *Chem. Rev.* **94,** 569 (1994).
19. J. J. Hastings and O. W. Howarth, *J. Chem. Soc., Dalton Trans.* 209 (1992).
20. H. Okamoto, A. Ishikawa, and T. Kudo, *Bull. Chem. Soc. Jpn.* **62,** 2723 (1989).
21. M. F. Daniel, B. Desbat, J. C. Lassegues, B. Gérand, and M. Figlarz, *J. Solid State Chem.* **67,** 235 (1987).
22. J. Gopalakrishnan, G. N. Subbanna, and N. S. Bhuvanesh, *Chem. Mater.* **6,** 373 (1994).
23. L. Dupont, D. Larcher, F. Portemer, and M. Figlarz, *J. Solid State Chem.* **121,** 339 (1996).
24. R. S. Roth and J. L. Waring, *J. Res. Natl. Bur. Stand.* **70A,** 281 (1966).
25. E. Salje, *Acta Crystallogr., A* **31,** 360 (1975).
26. I. R. Beattie and T. R. Gilson, *J. Chem. Soc. A* 2322 (1969).
27. F. Harb, B. Gérand, G. Nowogrocki, and M. Figlarz, *Solid State Ionics* **32–33,** 84 (1989).